IMPACT DAMAGE AND HYGROTHERMAL EFFECTS ON FATIGUE BENDING STRENGTH OF ORTHOTROPY COMPOSITE LAMINATES

Kwang-Hee Im[1], Jae-Woung Park [12] and In-Young Yang [13]
[1] Factory Automation Research Center for Parts of Vehicles
[2] Department of Naval Arch. and Ocean Engineering
[3] School of Mechanical Engineering
Chosun University, 375 Sosok-dong, Dong-gu
Kwangju 501-759, Korea

INTRODUCTION

Currently the importance of carbon-fiber reinforced plastics (CFRP) in both space and civil aircraft, which require superior stiffness and strength, has been generally recognized, and CFRPs are widely used due to the ultimate light weight to weight ratios compared to conventional metallic materials.

Unfortunately, CFRP laminates are brittle for dynamic loadings, particularly impact loading[1], which can significantly reduce their properties, and therefore the impact problems of composites are becoming important. A dropped wrench, bird strike[2] or runway debris can generate localized delaminated areas of foreign object damage (FOD)[3] by an impact which is frequently difficult to detect with the naked eye. Innocuous though this damage may seem in the stacking plates, it can result in premature catastrophic failure due to the decreasing strength caused by impact loading. Also deformation to the CFRP composite laminates is also possible with change of temperature and absorption of moisture[4] due to susceptiblility to hygrothermals, especially on the matrix material. Such hygrothermals can result in the presence of deformation in composite laminates, for example, interface properties which indicate the static and fatigue bending strength of the CFRP laminates[5].

Recently fatigue tests are widely performed using FRP laminates and notched laminates in the case of FRP members subjected to cycle loadings. Rotem[6] and Smith[7-8] have studied only the decreasing relationships of fatigue strength using composites under cycle loadings. And in the case of composite laminate subjected to hygrothermals, decreasing phenomena of residual strength have been studied[9].

Therefore, this paper attempts to evaluate the residual fatigue bending strength of laminates through a three-point bending fatigue test, to investigate moisture absorption characteristics on the fatigue bending strength under hygrothermals and to confirm failure mechanisms based on damage development.

MOISTURE-ABSORBTION THEORY

If the moisture diffusion is applied to the infinite-flat plate on assumption that the moisture diffusion is through the thickness to Equation (4), Fick's equation becomes as follows[10];

$$D_z \frac{\partial^2}{\partial z^2} M = \frac{\partial M}{\partial t} \tag{1}$$

where M is the moisture concentration, D_z is the moisture diffusion coefficient to Z-direction and t is the time (sec).

Boundary conditions of Equation (1) are as follows;

$$\begin{aligned} M &= M_0 \quad at \quad t \leq 0 \text{ and } 0 < z < h \\ M &= M_\infty \quad at \quad t > 0 \text{ and } z = 0,\ z = h \end{aligned} \tag{2}$$

where h is the thickness of laminates and z is the thickness direction of laminates.

The solution to Equations (1) and (2) is given as follows;

$$\frac{M - M_0}{M_\infty - M_0} = 1 - \frac{4}{\pi} \sum_{j=0}^{\infty} \left\{ \frac{1}{2j+1} \sin \frac{(2j+1)\pi z}{h} \exp\left[-\frac{\pi^2 D\, t}{h^2} (2j+1)^2 \right] \right\} \tag{3}$$

where M is the moisture absorption rate of laminates at an arbitrary time, M_∞ is the moisture saturation rate and M_0 is the initial moisture rate.

The laminates are weighed to determine the moisture content which is the total mass of the absorbed moisture divided by the dry weight of the laminates. The moisture content is in fact the same as the average specific moisture concentration $\overline{M}$ defined by;

$$\overline{M} = \frac{1}{h} \int_0^h M \, dz \tag{4}$$

Substituting Equation (3) into Equation (4) and noting that

$$\begin{aligned} \overline{M} &= M_0 \quad \text{for} \quad t = 0 \\ \overline{M} &= M_\infty \quad \text{for} \quad t = \infty \end{aligned} \tag{5}$$

We obtain from Equations (3) and (4) for short times an approximation can be obtained as follows;

$$\frac{\overline{M} - M_0}{M_\infty - M_0} = 4 \left(\frac{Dt}{\pi h^2} \right)^{\frac{1}{2}} \qquad (6)$$

Also, we can determine the moisture diffusion coefficient D from Equation (6) as;

$$D = \frac{\pi}{16} \left(\frac{\overline{M_2} - \overline{M_1}}{M_\infty - M_0} \right)^2 \left(\frac{h}{\sqrt{t_2} - \sqrt{t_1}} \right)^2 \qquad (7)$$

where h is the thickness (mm), $\overline{M}$ is the moisture absorbtion rate, M_0 is the initial absorbtion moisture rate, M_∞ is the moisture saturation rate and t is the time (sec).

EXPERIMENTAL METHOD

The laminates of the specimens were manufactured from one-directional prepreg sheets of T300-3000 carbon fibers. Its lay-up, stacked with 16 plies is $[0_4 / 90_4]_s$. Test specimens were prepared with dimensions 40mm × 180mm × 2.5mm (width × length × thickness).

The test fixture consisted of two steel plates and two rubber plates. A steel ball 5mm in diameter (0.5g) was impacted on the specimen by using compressed air. The velocity of the steel ball was measured just before impact by determining the time taken for it to pass two fine laser beams located a known distance (10mm) apart. After impact, the delamination of specimen interfaces was assessed using an ultrasonic microscope (Olympus UH100 with the range of 30MHz). Fatigue three-point bending tests are periodically interrupted for the impact-induced progressive damage from the fixture and the test is performed again. To examine residual bending fatigue strength of the specimen subjected to impact damages and to observe the damage growth in the specimens, a fatigue three-point bending test was carried out. Fig. 1(a) shows the fixture attached to the universal testing machine (Instron 8501) for the experiments of impacted-side tension and compression, respectively. Also, static and fatigue bending tests were carried out under the hygrothermals according to moisture absorbtion contents (0%, 0.2%, 0.7%, 1.5%). Fig. 2 shows the schematic of the three-point bending fatigue test under water. Distilled water at a temperature of 55℃ was used to accelerate the moisture absorbtion rate.

The fracture bending stresses were measured on the assumption that the specimen were homogeneous isotropic materials[11] because the stresses of CFRP laminates are linearly proportional to strain up to the point of rupture.

The fracture bending stress equation is as follows:

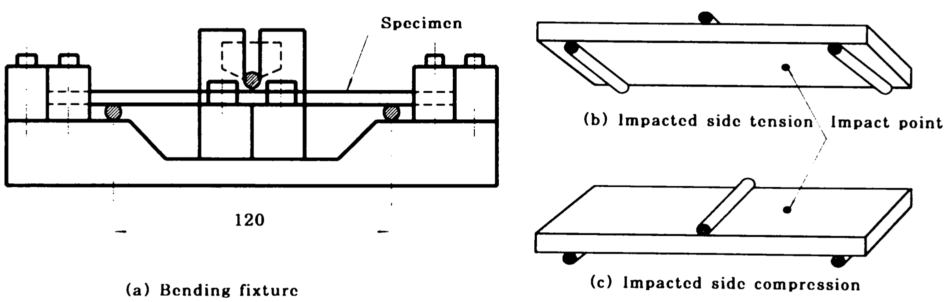

Fig. 1 Specimen supporting fixture for three-point bending test.

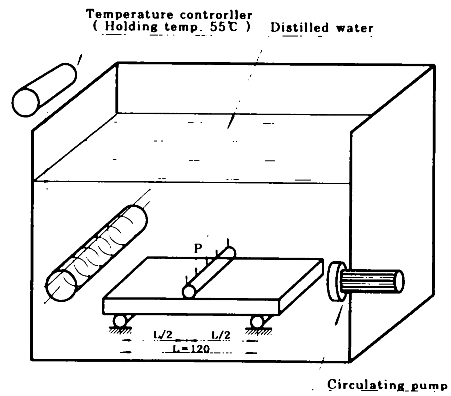

Fig. 2 Test arrangement of three-point bending fatigue test under water

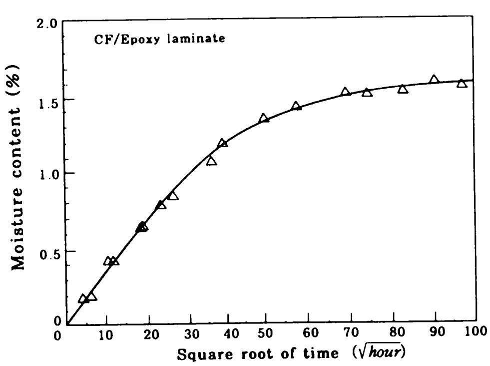

Fig. 3 Moisture content as a function of time under hygrothermals

$$I = \frac{bd^3}{12}, \qquad \sigma = \frac{(Pl/4)(d/2)}{I} = \frac{3PL}{2bd^2} \tag{8}$$

where σ is the bending stress (Pa), **P** is the maximum loading at fracture (N), **L** is the length of span (m) and **I** is the moment of inertia (m^4).

DISCUSSION AND RESULTS

Moisture Absorption Behavior under Hygrothermals

To investigate the influence of moisture content on fatigue bending strength when the composite laminates are subjected to hygrothermals, static and fatigue bending strengths of laminates are estimated according to the moisture content. Fig. 3 shows the moisture content with the variation of time. Rapid moisture content diffusion appears at the initial time, but with time the moisture-content diffusion slows. The moisture content diffusion was attained at the moisture saturation levels.

Observation of Progressive Damage from Impact Damages

In the case of impact-induced CFRP laminates subjected to cyclic loadings, initial impact damage in the interfaces is observed by using the SAM to build up the failure mechanisms and impact-damaged growth is observed in every specified cycle until fractured.

Figure 4 shows the damage growth direction in the case of impacted-side compression, and Fig. 4(a) and (b) indicate the delamination shapes after 0 and 20,000 cycles, respectively. Fig. 4 shows that fracture is propagated from the transverse crack generated near the impact point in the case of impacted-side compression and eventually fracture is generated along the transverse crack after 20,600 cycles.

Interrelations Between Residual Fatigue Bending Strength and Impact Damages vs. Moisture Content

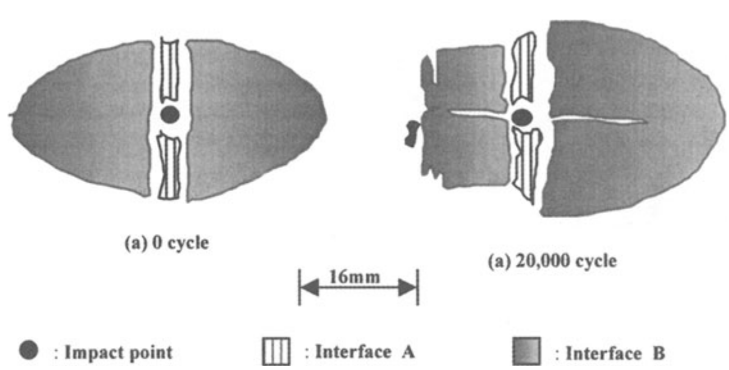

Fig.4 Progressive damage during fatigue bending test when the impacted side is compressed

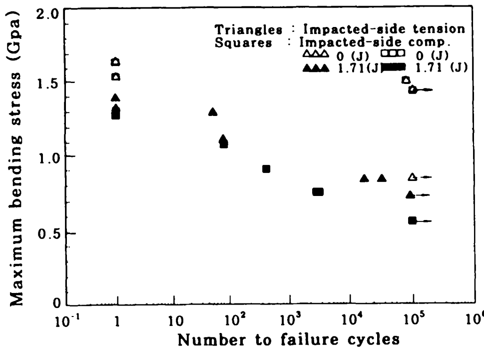

Fig. 5 Residual fatigue bending strength of damaged specimen

Figure 5 shows the fatigue strength in impacted-side compression decreased more than that in impacted-side tension because matrix cracks affect the fatigue bending strength, which were generated at an impact point. From Figrure 6, the rapid strength decreasing phenomena appear at approximately 0.2% if compared with those of non-moisture conditions. Even through the moisture rate increases, phenomena of decreasing strength do not occur.

Figure 7 shows the residual fatigue bending strength under the hygrothermals (0%, 0.2%, 0.7%, and 1.5% moisture content). Especially, at a moisture rate of approximately 0.2%, fatigue bending strength decreases greatly about 10% compared with the static bending strength because the moisture affects the matrix along the fibers.

Mechanism Failure from Impact-Induced Damages

Fig. 8(a) shows in detail the fracture growth modes in consideration of shear stresses, tension and compression in the plane. When the transverse cracks extend in the tension direction in these modes, opening displacement becomes greater, and when the cracks extend in the compression direction, closing phenomena occur. Thus, because the opening displacements on the tension side (modes Ⅰ+Ⅱ) are higher than those on the

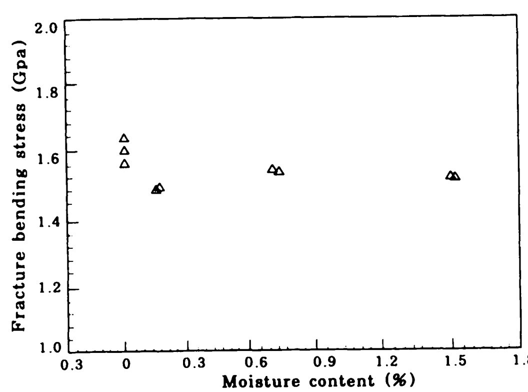

Fig. 6 Relation between fracture bending stress and moisture content

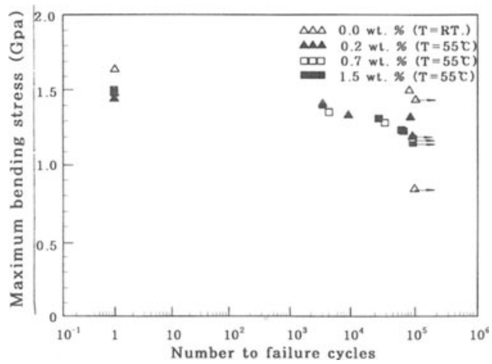

Fig.7 Residual fatigue bending strength variations according to moisture absorbtion contents

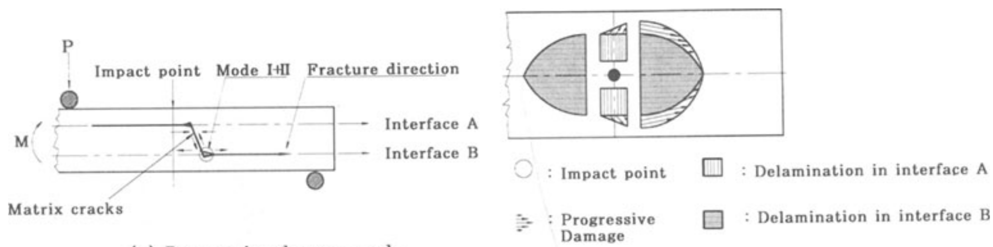

(a) Progressive damage mode

(b) Progressive damage direction

Fig.8 Damage mechanism during fatigue bending test when the impacted side is compressed

compressure side, delamination on the tension side can easily be extended. Thus, as shown in Fig. 8, the moment becomes greater because the radius of curvature at the fracture starting point was smaller in the case of impacted-side tension than in the case of impacted-side compression from the impact point.

CONCLUSIONS

The conclusions are as follows: It has been found that the phenomenon decreasing of residual fatigue bending strength in the case of impacted-side compression appear greater than those in the case of impacted-side tension for the orthotropic composite laminates. In the case of impacted-side compression, fracture is propagated from the transverse crack generated near the impact point. At approximately 0.2% of moisture content, the phenomens of rapid strength decrease appear and the strength variations do not occur at a moisture content of over 0.2%. It is thought that impact-induced damages and hygrothermals have an affect on the phenomena of residual fatigue strength decrease to some degree.

REFERENCES

1. T. Tanaka, T. Kurokawa, etc., 1989, "Damage and Residual Bending Strength of Graphite/Epoxy Composite Laminates Subjected to Normal Impact", *Journal of the Japan Society for Aeronautical & Space Sciences*, Vol. 37, No. 25, pp. 29-36.
2. C. C. Ma., Y. H. Huang, and M. J. Chang, 1991, "Hygrothermal Effect on the PEEK/C.F. and PPS/C. F. under Impact Loading(I)", *ANTEC*, pp. 2029-2096.
3. T. Takeda, 1985, "Impulsive Response and Fracture of Composites (I)", *Journal of the Japan Society for Composite Materials*, Vol. 11, No. 4, pp. 151-161.
4. S. W. Tsai and H. T. Hahn, 1980, "Introduction to Composite Materials", Technomic Publishing Co., Inc., pp. 329-376.
5. K. D. Challenger, 1986, "The Damage Tolerance of Carbon Fiber Reinforced Composites" A Workshop Summary, *Composite Struct.*, pp. 295-318.
6. A. Rotem and H. G. Nelson, 1990, "Residual Strength of Composite Laminate Subjected to Tensile-Compressive Fatigue Loading", *Journal of Composites Technology & Research,* Vol. 12, No. 2, pp. 76~84.
7. B. W. Smith and R. A. Grove, 1987, "Determination of Crack Propagation Directions in Graphite/Epoxy Structures", *Composites and Metals,* ASTM. STP. 948, pp. 154-173.
8. K. H. Im, J. K. Sim and I. Y. Yang, 1996, "Impact Damages and Residual Bending Strength of CFRP Composite Laminates Subjected to Impact Loading", *KSME International Journal,* Vol. 10, No. 4, pp. 423-434.
9. J. S. Sirkis, C. C. Chang and B. T. Smith, 1994, "Low Velocity Impact of Optical Fiber Embedded Laminated Graphite/Epoxy Panels. Part I : Macro-Scale", *Journal of Composite Materials,* Vol. 28, No. 14, pp. 1347~1371.
10. O. Ishai and V. Arnon, 1978, "Instantaneous Effects of Internal Moisture Conditions on Strength of Glass-Fiber-Reinforced Plastics", ASTM, pp. 267~276.
11. L. E. Malvern, C. T. Sun and D. Liu, 1989, "Delamination Damage in Central Impacts at Subperformation Speeds on Laminated Kevlar/Epoxy Plates", *ASTM. STP.* 1012, pp. 387~405.